Molecular Cell *21*, 617–628, March 3, 2006 ©2006 Elsevier Inc. DOI 10.1016/j.molcel.2006.01.028

A Transient Heterochromatic State in *Xist* Preempts X Inactivation Choice without RNA Stabilization

Bryan K. Sun,[1,2,3] Aimée M. Deaton,[1,2,3] and Jeannie T. Lee[1,2,3,*]
[1] Howard Hughes Medical Institute
[2] Department of Molecular Biology
Massachusetts General Hospital
Boston, Massachusetts 02114
[3] Department of Genetics
Harvard Medical School
Boston, Massachusetts 02114

Summary

X chromosome inactivation (XCI) depends on a noncoding sense-antisense transcript pair, *Xist* and *Tsix*. At the onset of XCI, *Xist* RNA accumulates on one of two Xs, coating and silencing the chromosome in *cis*. The molecular basis for monoallelic *Xist* upregulation is not known, though evidence predominantly supports a posttranscriptional mechanism through RNA stabilization. Here, we test whether *Tsix* RNA destabilizes *Xist* RNA. Unexpectedly, we find that *Xist* upregulation is not based on transcript stabilization at all but is instead controlled by transcription in a sex-specific manner. *Tsix* directly regulates its transcription. On the future inactive X, *Tsix* downregulation induces a transient heterochromatic state in *Xist*, followed paradoxically by high-level *Xist* expression. A *Tsix*-deficient X chromosome adopts the heterochromatic state in pre-XCI cells. This state persists through XCI establishment and "reverts" to a euchromatic state during XCI maintenance. We have therefore identified chromatin marks that preempt and predict asymmetric *Xist* expression.

Introduction

Antisense transcripts are found in abundance throughout the mammalian genome (Lavorgna et al., 2004; Shendure and Church, 2002; Yelin et al., 2003) and appear to be overrepresented at epigenetically regulated loci (Lee, 2003; Sleutels and Barlow, 2002). Among imprinted domains, an intriguing feature shared by many antisense transcripts is a monoallelic expression pattern inversely correlated with their sense counterparts. This fact has prompted the increasingly popular view that antisense transcription may be involved in regulating asymmetric gene expression. The phenomenon of XCI provides a paradigm for understanding sense-antisense pairs. During XCI, one of two X chromosomes is transcriptionally silenced in females, equalizing the dosage of X linked genes between females (X/X) and males (X/Y) (Lyon, 1961). At the onset of XCI, the noncoding X-inactive specific transcript (*Xist*) is upregulated from one of two Xs, coating and silencing the chromosome in *cis* (Brockdorff et al., 1992; Brown et al., 1992). *Tsix*, its noncoding antisense partner, antagonizes *Xist*'s ability to initiate silencing (Lee and Lu, 1999; Sado et al., 2001). Thus, XCI is regulated by the opposing action of sense and antisense genes in *cis*.

How does this interplay result in asymmetric silencing of the Xs? In principle, *Tsix* could regulate *Xist* at either the transcriptional or posttranscriptional levels. Two early studies used nuclear run-on analysis and measurements of steady-state levels to argue that *Xist* is posttranscriptionally regulated by RNA stabilization rather than by increased transcriptional rate (Panning et al., 1997; Sheardown et al., 1997). According to this model, the switch from low to high levels of *Xist* occurs through stabilizing the RNA on the future inactive X (Xi) by factors produced only during cell differentiation and the onset of XCI. These findings have directed the search for mechanisms that trigger *Xist* stability on one X without affecting that on the other.

The subsequent discovery of antisense transcription at the *Xist* locus led to the hypothesis that an antisense RNA might control *Xist* stability (Lee et al., 1999). The pattern of sense and antisense expression supports a role for *Tsix* in negatively regulating *Xist*: *Tsix* expression is biallelic before the onset of XCI but is downregulated on one X just before the upregulation of *Xist* on that chromosome. Genetic manipulations that block *Tsix* cause *Xist* RNA to be upregulated exclusively from the *Tsix*-deficient chromosome (Lee and Lu, 1999; Luikenhuis et al., 2001; Sado et al., 2001; Shibata and Lee, 2004). Conversely, forced or induced *Tsix* expression prevents *Xist* upregulation in *cis* (Luikenhuis et al., 2001; Stavropoulos et al., 2001). Thus, in some way, *Tsix* transcription or RNA controls the expression of *Xist*.

Two recent studies have proposed that modulation of *Xist* chromatin structure may play a role in how *Tsix* regulates *Xist*. One study has examined how the chromatin at the *Xist* promoter responds to a truncation of *Tsix* transcription in later-stage embryos (Sado et al., 2005). During the "maintenance phase" of XCI, they observe greater DNase I hypersensitivity, increased histone H4 acetylation, and decreased histone H3-K27 methylation at the *Xist* promoter, suggesting that the loss of *Tsix* leads to open chromatin structure at *Xist* in *cis*. In agreement, a second study finds increased H3-K4 dimethylation and RNA Pol II binding at the active *Xist* promoter in differentiated cells (Navarro et al., 2005). These studies imply that *Xist* may also be regulated at the transcriptional level. However, because the analyses are undertaken predominantly in post-XCI differentiated cells (maintenance phase), it is currently not known whether these chromatin marks precede *Xist* expression and are required to establish the pattern of XCI. Therefore, the idea that *Tsix* may regulate *Xist* transcription remains an open question.

We now investigate how high-level, asymmetric *Xist* levels are achieved. First, we examine whether *Tsix* directly affects *Xist* RNA stability. In the course of analysis, we were surprised to find that *Xist* RNA is not regulated by stabilization but is instead regulated through promoter upregulation. Further investigation reveals how *Tsix* controls the establishment of an asymmetric

*Correspondence: lee@molbio.mgh.harvard.edu

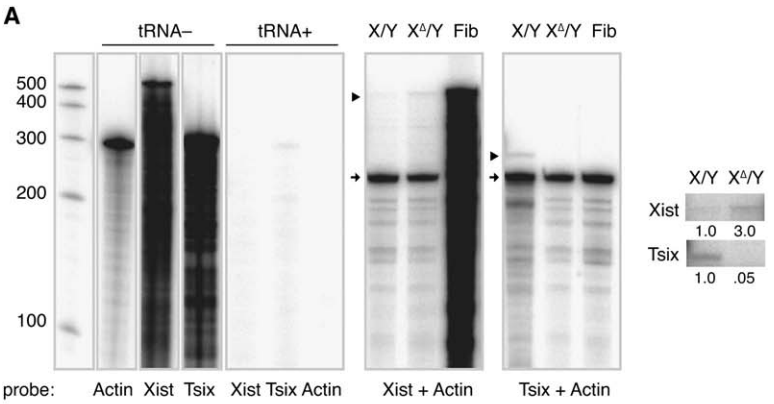

B

	undifferentiated	differentiated
X/Y	1.0	ND
X^{Δ}/Y	1.6 ± 0.1	ND
X/X	1.0	31.1 ± 1.2
X^{Δ}/X	5.9 ± 0.6	ND

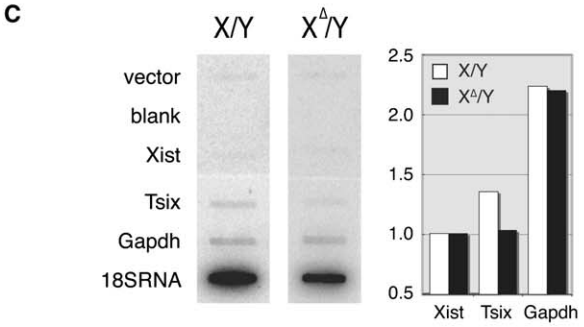

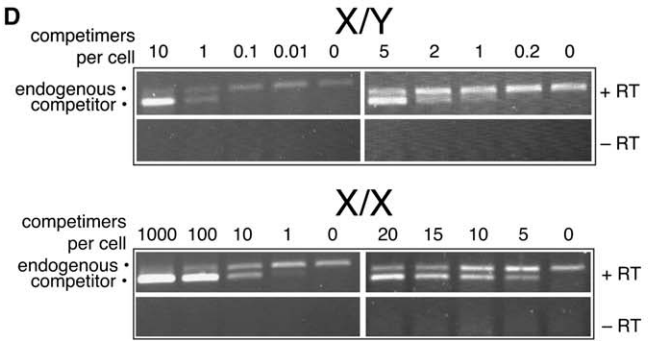

Figure 1. Relationship between *Xist* and *Tsix* Steady-State RNA and Transcription Levels

(A) RNase protection assay. Arrowheads denote protected *Xist* and *Tsix*; arrows show protected *β-Actin*. Female fibroblasts (Fib) were run as a positive control for *Xist* and negative control for *Tsix*. Inset focuses on the protected *Xist* and *Tsix* fragments in ES cells. Abundance of each transcript shown relative to wild-type (X/Y = 1).

(B) Steady-state levels of *Xist* determined by real-time RT-PCR relative to X/X or X/Y ± standard deviation of triplicate measurements. ND, not determined.

(C) Nuclear run-on assays. Probe intensities were normalized to *18SRNA* then plotted relative to background (vector = 1.0).

(D) Competitive RT-PCR to determine *Xist* RNA copy number in pre-XCI ES cells. Left panels represent 10-fold dilutions. Right panels represent finer dilution series.

chromatin state, including formation of histone marks that preempt and predict monoallelic *Xist* induction.

Results

Effect of *Tsix* on *Xist* Transcription and Steady-State Levels

Levels of *Xist* RNA prior to the onset of XCI have been correlated with the probability that a given X chromosome will be chosen for inactivation (Nesterova et al., 2003). To determine whether *Tsix* affects *Xist* steady-state levels prior to the onset of XCI, we performed RNase protection assays on undifferentiated wild-type (wt) and *Tsix* mutant male lines (J1 and CG7 lines as described in Lee and Lu [1999]), hereafter referred to as X/Y and X^{Δ}/Y (Figure 1A). We compared the amount of each transcript produced from a single *Xist* locus. In the X^{Δ}/Y line, *Tsix* was reduced to ~5% of wt levels whereas *Xist* increased 2- to 3-fold (Figure 1A).

To confirm the RNase protection results, we performed real-time RT-PCR on male and female wt and heterozygous *Tsix* mutant lines (16.6 and 3F1 lines as described in Lee and Lu [1999]), hereafter referred to as X/X and X^{Δ}/X. *Xist* RNA levels were elevated ~1.6-fold in the X^{Δ}/Y mutant and ~6-fold in the X^{Δ}/X mutant compared to the corresponding wt lines (Figure 1B).

The sex-specific difference in *Xist* derepression may indicate that the loss of *Tsix* has a greater effect on *Xist* levels in female cells or that the X^{Δ}/X culture contained partially differentiated cells with upregulated *Xist*. As observed previously (Lee and Lu, 1999; Morey et al., 2001), the increased amounts of *Xist* RNA in the mutant cells were not sufficient to cause X inactivation, indicating that required factors were missing. These results demonstrated that the steady-state level of *Xist* RNA is inversely proportional to *Tsix* RNA in pre-XCI cells, consistent with the idea that *Tsix* might destabilize *Xist*.

However, in female embryonic stem (ES) cells undergoing XCI during differentiation into embryoid bodies (EBs), the steady-state *Xist* levels increased at least 31-fold (Figure 1B). Therefore, the 6-fold effect observed upon deleting *Tsix* accounted for only a fraction of the 31-fold effect. Thus, if *Tsix* regulated *Xist* through RNA stability, this posttranscriptional mechanism alone cannot explain the magnitude of *Xist* upregulation during XCI. We therefore asked whether *Xist* may also be regulated by transcription by performing nuclear run-on assays to look for transcriptional rate differences between $Tsix^{+}$ and $Tsix^{-}$ cells (Figure 1C). As expected, antisense transcription was readily detected in X/Y cells and was reduced in X^{Δ}/Y. However, *Xist* transcription was indistinguishably low in X/Y and X^{Δ}/Y as assayed by various strand-specific probes (Figure 1C and data not shown).

Our results contrasted with previous nuclear run-on experiments, which observed sense, but not antisense, transcripts (Panning et al., 1997; Sheardown et al., 1997). One significant difference is that we used single-stranded *Xist* probes, whereas previous studies (preceding the discovery of *Tsix*) predominantly used double-stranded probes. With bidirectional transcription in this region and *Tsix* at 10- to 100-fold greater levels than *Xist* in pre-XCI cells (Shibata and Lee, 2003), double-stranded probes would in retrospect have favored detection of the antisense RNA. We thus conclude that pre-XCI ES cells predominantly transcribe *Tsix* and show very little, if any, *Xist* transcription.

Absolute Copy Numbers of *Xist* RNA

Although our nuclear run-on assay did not detect *Xist* transcription, sense RNA has been observed by the more sensitive RT-PCR and RNA FISH techniques (Beard et al., 1995; Lee et al., 1999). We next estimated the absolute *Xist* RNA copy numbers in pre-XCI cells by competitive RT-PCR in which each RNA preparation was "spiked" with a known quantity of competitor RNA that can be distinguished from the endogenous RNA by a small deletion of 38 bases (Figure 1D). Because both endogenous and competitor RNAs were subject to the same isolation process and reverse transcription, this assay provided a realistic calculation of the absolute copy number. By comparing endogenous levels against a serial dilution series of competitor RNA, we derived the RNA copy number from the "equivalence point" at which endogenous and competitor molecules showed a 1:1 representation. The analysis showed that each X/Y ES cell had three to four copies of *Xist* RNA, whereas an X/X cell had approximately ten copies. Thus, each *Xist* allele produces very low quantities of *Xist* RNA at the steady state before the onset of XCI.

After differentiating into EBs, X/X cells upregulated *Xist* RNA by at least 31-fold (Figure 1B). By inference, each Xi must be coated by at least 300 copies of *Xist* RNA. We conclude that *Xist* RNA is present at approximately ten copies in pre-XCI females and accumulates >300 copies at the onset of XCI—a conclusion that is within range of previous estimates (Buzin et al., 1994).

Xist Is Not Regulated by RNA Stabilization

Previously, observations of high transcriptional rates in the absence of significant RNA accumulation led to the idea of an unstable *Xist* RNA in pre-XCI ES cells. This idea had been supported by half-life ($t_{1/2}$) measurements showing a $t_{1/2}$ increase from 0.5 hr in ES cells to 6 hr after XCI (Panning et al., 1997; Sheardown et al., 1997). We repeated the RNA $t_{1/2}$ experiments with a strand-specific technique to distinguish *Xist* and *Tsix* stabilities. We treated cells with Actinomycin D for 0–10 hr to inhibit transcription, isolated RNA at 1–2 hr time points, and then quantified the RNA by strand-specific, real-time RT-PCR.

We first tested pre-XCI male and female ES cells and found that the $t_{1/2}$ of the sense transcript was ~6 hr in both (Figure 2A), contrasting with the 0.5 hr $t_{1/2}$ previously reported (Panning et al., 1997; Sheardown et al., 1997). Upon cell differentiation, *Xist* RNA stability did not change significantly (Figure 2B). The same assay performed on primary female fibroblasts yielded a $t_{1/2}$ of 3–4 hr (data not shown). Therefore, *Xist* RNA stability did not vary substantially between cells in the pre- and post-XCI states. Furthermore, the absence of *Tsix* RNA did not alter the $t_{1/2}$, as X/Y and X^{Δ}/Y cells both exhibited a $t_{1/2}$ of ~6 hr (Figure 2C). In X^{Δ}/X female cells, the $t_{1/2}$ was ~3.5 hr (Figure 2D), a value consistent with what is observed in female fibroblasts (data not shown). This demonstrated that *Tsix* RNA had no dramatic effect on *Xist* RNA stability.

We next tested *Tsix* $t_{1/2}$ with the identical primer pair in real-time RT-PCR but carried out the first-strand reaction with the opposite strand primer. Interestingly, *Tsix* RNA $t_{1/2}$ was <1 hr in undifferentiated female and male ES cells (Figure 2E and data not shown), implying a much lower stability of *Tsix* RNA relative to that of *Xist*. Thus, the instability formerly attributed to *Xist* RNA actually reflected the instability of *Tsix* RNA. Our results are consistent with the measurements of stable $t_{1/2}$ (5–6 hr) in mouse transgenic *Xist* (Wutz and Jaenisch, 2000) and human *XIST* RNA (Clemson et al., 1998). We conclude that the initiation of XCI is not regulated by a switch from unstable to stable *Xist* RNA, that *Xist* RNA is strikingly stable across all developmental stages, and that *Tsix* RNA had little effect on its overall stability. The antagonistic properties of *Tsix* must therefore depend on other mechanisms.

Xist Upregulation Occurs through Increased Transcription

We next considered the possibility that *Xist* upregulation may be based on transcription by testing a 540 bp *Xist* P1 promoter in a luciferase reporter assay in pre- and post-XCI cells. After stably integrating a transgene into X/Y and X/X ES cells, we pooled 25–100 colonies, differentiated them in triplicate, and measured luciferase levels at various time points. In X/Y cells, *Xist* promoter

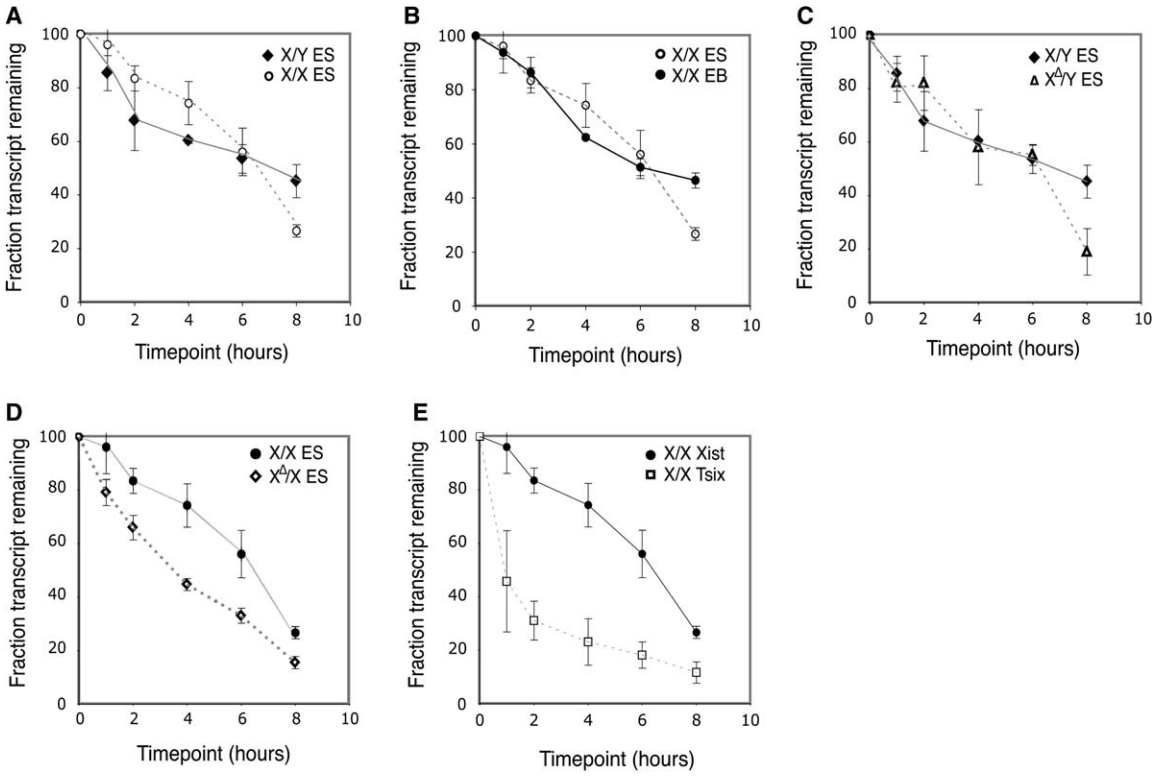

Figure 2. *Xist* RNA Upregulation Is Not Mediated by RNA Stabilization

(A–D) *Xist* RNA half-life measured by strand-specific, real-time RT-PCR after Actinomycin D treatment. Experiments were performed in replicate, and cycling reactions in triplicate. Points represent averages from duplicate experiments ± standard error of the mean.

(E) *Tsix* RNA is much less stable than *Xist*. To detect antisense RNA, the oppositely oriented first strand primer was used in the RT reaction.

activity was low in pre-XCI cells and remained low during differentiation, consistent with the lack of *Xist* RNA accumulation in male cells (Figure 3).

In X/X cells, the promoter activity was low in the pre-inactivation state but was upregulated during differentiation by 2- to 10-fold on average (Figure 3 and data not shown). Raw luciferase levels were significantly elevated over two independent promoterless-luciferase control pools, arguing that the observed transcriptional activity and induction was specific to the *Xist* promoter.

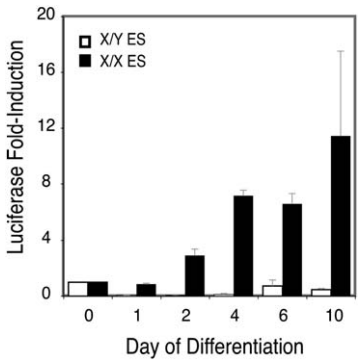

Figure 3. *Xist* Is Upregulated through Transcriptional Induction

An *Xist* promoter:luciferase transgene was stably integrated into ES cells. Cells were differentiated in triplicate, and normalized luciferase levels are plotted relative to day 0 ± standard deviation.

Clearly, however, the 2- to 10-fold increase does not fully account for the 31-fold increase in steady-state levels, suggesting that the 540 bp promoter fragment does not contain all the necessary elements to achieve full activation. We conclude that an increase in *Xist* transcription rate contributes significantly to RNA accumulation and this mechanism of upregulation is specific to X/X cells.

Evidence for RNA-Directed DNA Methylation at the *Xist* Promoter

We next examined if *Tsix* regulates asymmetric transcriptional expression of *Xist*. It has been shown that the *Xist* promoter is differentially methylated in somatic female cells. Correlating with the transcriptional status of each allele, the silent *Xist* promoter is methylated, whereas the active *Xist* promoter is unmethylated (McDonald et al., 1998). In undifferentiated female ES cells, however, the two promoters are mosaically methylated (Penny et al., 1996; Sado et al., 1996), indicating that functional methylation is differentiated on the two *Xist* alleles during XCI. Because *Tsix* is itself differentially expressed during the process of XCI, we examined whether it influenced the establishment of differential *Xist* promoter methylation.

We performed allele-specific restriction enzyme methylation analysis at two promoter positions, MluI and SacII, in differentiating ES cells (Figure 4A). In X/X and X^{Δ}/X cells, the two Xs originated from different

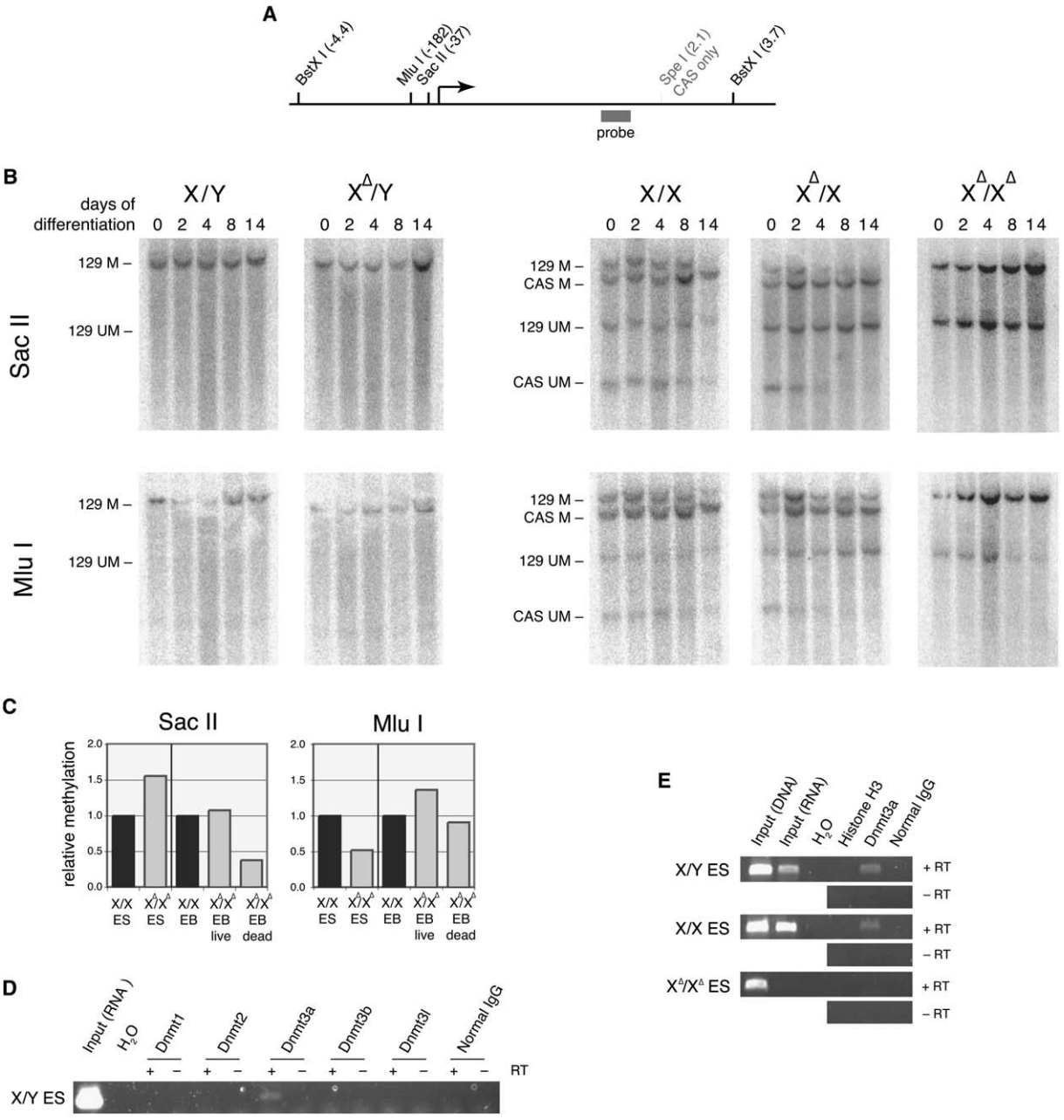

Figure 4. Relationship of *Tsix* to Establishment of *Xist* Promoter Methylation

(A) Scheme for methylation-sensitive restriction analysis by Southern blot.

(B) Allele-specific, methylation-sensitive restriction analysis of *Xist* promoter during differentiation. CAS, *M. castaneus* allele. Abbreviations: M, methylated; UM, unmethylated.

(C) Methylation-sensitive PCR assay on live adherent cells and dead detached cells on d8. Amplification threshold differences (ΔCt) between undigested and SacII/MluI-digested DNA were used to quantitate methylation.

(D) RNA-ChIP with a panel of DNA methyltransferases (d0 ES).

(E) *Tsix* RNA-ChIP against *Dnmt3a* and histone H3 (d0 ES).

mouse strains (X_{129} and X_{cas}, from 129 and *Mus castaneus*, respectively) and could therefore be distinguished by single nucleotide polymorphisms (SNP). Interestingly, *Xist* promoter methylation differed significantly between males and females. In X/Y, the *Xist* promoter was fully methylated before and after differentiation (Figure 4B), agreeing with a previous report that *Xist* methylation is already established in male ES cells (Norris et al., 1994). The absence of *Tsix* did not affect methylation in males (X^{Δ}/Y; Figure 4B), correlating with a lack of XCI phenotype in *Tsix*-deficient males (Lee and Lu, 1999).

In contrast, female cells exhibited different methylation patterns before and after XCI. In pre-XCI cells, the promoter was only partially methylated and this methylation could occur on either X_{129} or X_{cas} (Figure 4B). At

the onset of XCI, *Xist* was progressively methylated on X_{cas} and less methylated on X_{129}, consistent with a natural *Xce* skewing effect in the 16.6 line (Johnston and Cattanach, 1981; Lee and Lu, 1999). The pattern of methylation reached equilibrium on day (d) 14. To determine whether *Tsix* affected methylation patterns, we examined X^{Δ}/X differentiation. Interestingly, although d0 patterns were identical to that of wt, cell differentiation led to a more rapid and extreme skewing of *Xist* methylation to favor the *castaneus* allele, with methylation reaching equilibrium by d4, 10 days earlier than in wt. The methylation on X_{cas} correlated with the exclusive silencing of *castaneus Xist* in the X^{Δ}/X mutant (Figure 4B) (Lee and Lu, 1999). These results implied that *Tsix* may trigger *Xist* methylation.

Given this, the methylation state of the homozygous X^{Δ}/X^{Δ} mutant (ΔF10 [Lee, 2005]) was of particular interest. X^{Δ}/X^{Δ} cells lose mutual exclusion of XCI choice, with some EB cells displaying two active *Xist* loci, and therefore exhibit massive cell death during differentiation. Surviving cells display overtly random XCI, however (Lee, 2002). Southern blot analysis showed that the *Xist* promoter was partially methylated in pre-XCI X^{Δ}/X^{Δ} cells and became progressively more methylated from d2 to d14 (Figure 4B) (note: because both Xs are of 129 origin, they could not be distinguished).

At first, the ability of the X^{Δ}/X^{Δ} line to methylate *Xist* suggested that *Tsix* does not regulate methylation. However, given that >50% of X^{Δ}/X^{Δ} cells die during differentiation (Lee, 2005), we considered the possibility that X^{Δ}/X^{Δ} survivors were not representative of the population, because only attached, viable EB cells were included. We next harvested floating dead cells (trypan $blue^{+}$ fraction) during a 24 hr period from d7 to d8. Because DNA quantities were limited and might be fragmented by apoptosis, we carried out a methylation-sensitive PCR assay with SacII or MluI (Figure 4C). At both sites, the dead fraction was significantly undermethylated, with overall methylation comparable or less than what was observed in X/X cells. This was consistent with the idea that a failure of *Xist* promoter methylation on both Xs led to inappropriate *Xist* expression patterns in X^{Δ}/X^{Δ} cells. In contrast, the live fraction showed a wt level of DNA methylation. We therefore propose that *Tsix* induces functional DNA methylation at the *Xist* promoter and that this methylation maintains *Xist* repression.

Could *Tsix* RNA interact with DNA methyltransferases at the *Xist* promoter? To address this question, we performed RNA-chromatin immunoprecipitation (RNA-ChIP) in which we immunoprecipitated ES cell chromatin with antibodies against known DNA methyltransferases and tested for the presence of *Tsix* RNA (Figure 4D). Whereas *Dnmt1*, *Dnmt2*, *Dnmt3b*, and *Dmnt3l* did not associate with *Tsix* RNA, *Dnmt3a* was reproducibly found in a complex with *Tsix* RNA in both male and female ES cells (Figure 4E), consistent with *Dnmt3a*'s ability to de novo methylate *Xist* (Chen et al., 2003). The RNA-protein complex appeared specific, as it was not seen in the X^{Δ}/X^{Δ} line. Moreover, *Tsix* RNA did not associate with histone H3 (Figure 4E and Figure S1 available in the Supplemental Data with this article online), suggesting that the *Tsix* RNA-*Dnmt3a* complex was not simply due to its proximity to the *Xist* chromatin. We therefore propose that *Tsix* RNA activates *Dnmt3a* at the *Xist* promoter to silence *Xist* on the future Xa and that, in X^{Δ}/X^{Δ} cells, the loss of promoter methylation contributes to inappropriate *Xist* expression and cell death. Thus, *Xist* transcriptional silencing is in part regulated by *Tsix* RNA-directed DNA methylation at the promoter.

A Transient Heterochromatic State in *Xist* Preempts Transcriptional Induction

Does *Tsix* control other aspects of *Xist* chromatin structure? At the *Xic*, active and inactive *Xist* loci have been shown to reside in different chromatin environments, with the silent *Xist* allele associated with dimethylated H3-K9 (H3-2meK9) and trimethylated H3-K27 (H3-3meK27), and the active allele associated with dimethylated H3-K4 (H3-2meK4) (Goto et al., 2002; Navarro et al., 2005; Sado et al., 2005). However, it is currently not known whether they are a cause or consequence of asymmetric *Xist* expression, as analyses have been focused on post-XCI cells. Relevant to this, XCI can be genetically separated into three phases: a "pre-XCI phase" in which cells have not yet committed to inactivation (d0 ES cells), an *Xist*-dependent "establishment phase" during which counting, choice, and initiation of silencing take place, and then a "maintenance phase" in which the Xi is propagated independently of *Xist*. A priori, any causative histone mark must precede the onset of XCI.

To address this issue, we queried the chromatin structure at *Xist* during the various phases by ChIP analysis at the *Xist* promoter and gene body (Figure 5A). All analyses were carried out in 129/*castaneus* hybrid female cells so differences between the Xa and Xi could be detected, with one X serving as internal control for the other. We first tested H3-2meK9 but found that this mark was extremely low in all tested cells (data not shown), consistent with prior analysis (Rougeulle et al., 2004). This implied that this modification was not involved in the regulation of *Xist* or that its levels were below the detection limit. In contrast, H3-2meK4 levels showed dynamic changes. At the *Xist* promoter, total H3-2meK4 remained constant before and during XCI (Figure 5A). By fractionating the immunoprecipitated DNA by SNP-based allele-specific PCR (Figure 5B), we found that methylation was equal between the two *Xist* alleles in pre-XCI cells. The distribution became skewed toward the 129 allele in cells undergoing XCI and in post-XCI cells, a distribution that mirrored the naturally skewed *Xist* expression patterns in this hybrid line.

To determine the relationship of *Tsix* expression to H3-2meK4, we carried out ChIP in X^{Δ}/X cells. Interestingly, although deleting *Tsix* had little effect on the *Xist* promoter, it significantly decreased H3-2meK4 in the gene body. The decrease specifically took place on X_{129}, which carried the *Tsix* mutation. These results indicated that *Tsix*'s effect on *Xist* transcription does not depend on any ability to modulate H3-2meK4 at the promoter. This result contrasted with the conclusion of Navarro et al., who hypothesized that *Tsix* acts by modulating *Xist* promoter H3-K4 dimethylation ([Navarro et al., 2005] see Discussion). Although our data showed no evidence for a promoter effect in d0 cells, they did indicate that *Tsix* specifically affects H3-2meK4 levels in the *Xist* gene body. Consistent with what we observed

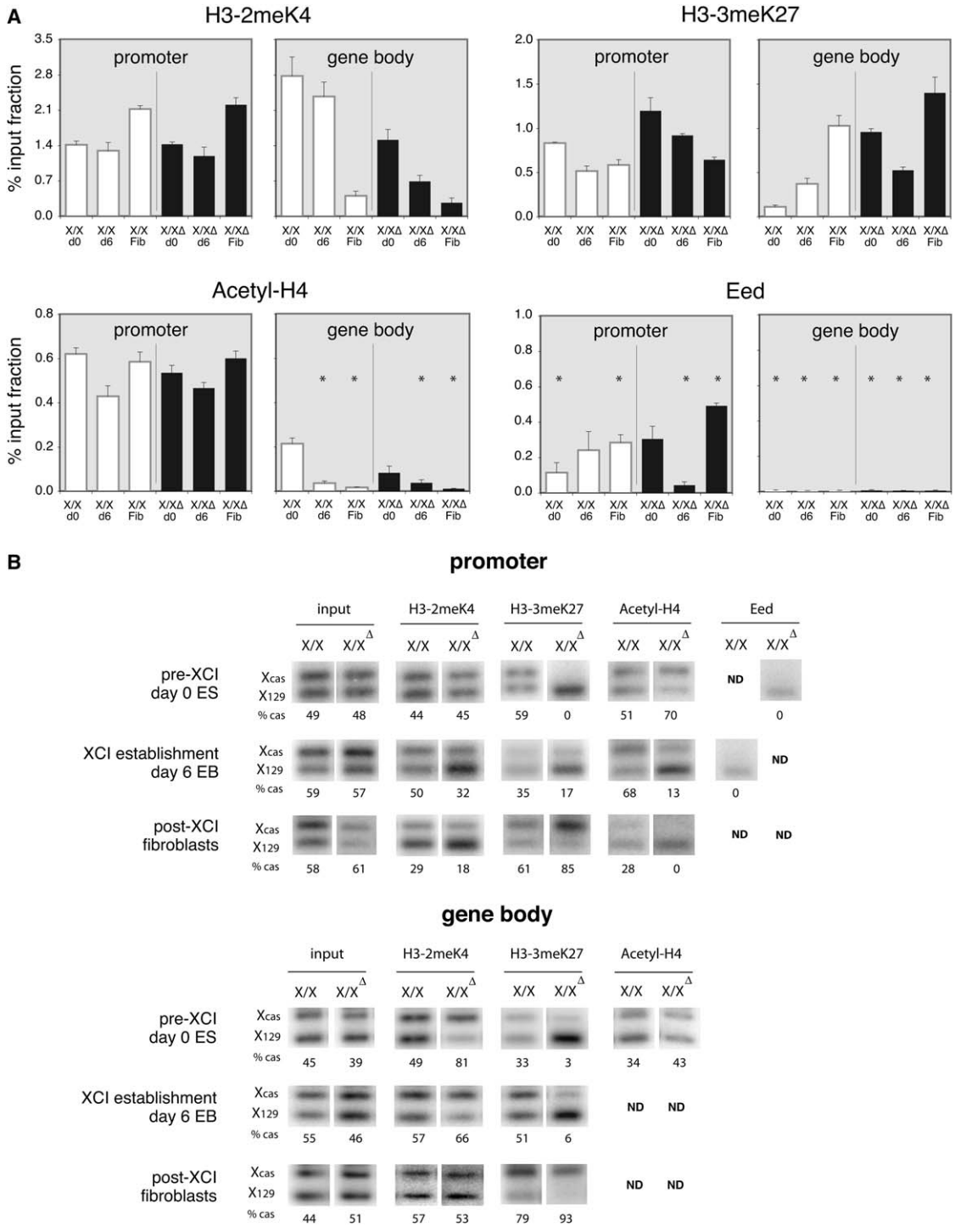

Figure 5. Loss of *Tsix* Leads to Preemptive Histone Modifications at the *Xist* Locus

(A) ChIP analysis of the *Xist* promoter and gene body. Each ChIP was repeated multiple times with consistent results. Immunoprecipitated products are graphed as a percentage of input chromatin, quantitated by real-time PCR ± standard deviation. Asterisks denote levels that did not consistently exceed normal IgG control levels (background).

(B) Allele-specific ChIP of immunoprecipitations from (A). The *Tsix* mutation in X^{Δ}/X is on the 129 X. ND, not determined.

in wt X/X cells, antisense expression paradoxically raised the level of H3-K4 dimethylation on the *Xist* allele that is destined to be repressed.

We next examined H3-3meK27 (Figures 5A and 5B). At the promoter, the H3-3meK27 levels were consistently measurable in wt X/X cells and were approximately equal on both alleles. At the onset of XCI, H3-3meK27 became asymmetric, as levels were reproducibly enriched on the *Xist* allele of the future Xi—the allele that was to become induced. This pattern of methylation was opposite of the

broadly accepted idea that H3-3meK27 occurs on silent alleles. To confirm these findings, we tested for the presence of *Eed*, a protein in the H3-K27 methyltransferase complex (Cao et al., 2002). Indeed, *Eed* was elevated on the 129 allele and correlated with the enrichment of H3-3meK27 (Figures 5A and 5B).

To test whether *Tsix* regulates H3-K27 methylation, we examined X^{Δ}/X cells (Figures 5A and 5B). Intriguingly, methylation occurred almost exclusively on X_{129}, the chromosome lacking *Tsix*. This further argued that the heterochromatic mark H3-3meK27 occurred on the *Xist* promoter and gene body of the future active allele. Importantly, this asymmetry was present prior to *Xist* induction and the onset of XCI and persisted through the establishment phase. Similar paradoxical findings were evident for histone H4 acetylation at the *Xist* promoter (Figures 5A and 5B). Taken together, these data suggested that *Tsix* expression promotes a euchromatic character in the *Xist* locus and that the loss of *Tsix* results in a heterochromatic state that preempts and predicts XCI patterns.

Finally, to address whether the heterochromatic state persisted into the maintenance phase, we examined histone marks in fibroblasts isolated from X/X and X^{Δ}/X mice. Unexpectedly, there was a complete inversion in the chromatin pattern. At the active *Xist* locus, while H3-2meK9 remained low (data not shown), H3-K4 became hyperdimethylated, H3-K27 became hypotrimethylated, and histone H4 became hyperacetylated (Figure 5B). These data are consistent with the recent findings in post-XCI cells (Navarro et al., 2005; Sado et al., 2005) and imply that the *Xist* chromatin pattern found in the XCI maintenance phase is established at later stages and does not establish or predict *Xist* expression.

Collectively, the ChIP analyses led us to several major conclusions. First, the chromatin at *Xist* exhibits dynamic changes in response to *Tsix*. Monoallelic loss of *Tsix* expression causes a transient and asymmetric heterochromatic state involving H3-2meK4, H3-3meK27, and histone H4 acetylation that precedes induction of *Xist* expression on the future Xi. We propose that this heterochromatic state underlies the initiation and establishment of asymmetric *Xist* expression but is not required after XCI transitions to an *Xist*-independent maintenance state.

Discussion

Xist Is Controlled by Transcription, Not RNA Stabilization

We have shown that *Xist* RNA is not regulated by RNA stabilization. Previous studies preceded discovery of *Tsix* and were likely confounded by the use of double-stranded probes (Panning et al., 1997; Sheardown et al., 1997). With *Tsix* RNA being more abundant, previous measurements may inadvertently have detected *Tsix* instead of *Xist*. Using strand-specific techniques, we have now demonstrated that *Xist* RNA $t_{1/2}$ is relatively unchanged throughout XCI and that transcriptional activation can at least partially account for *Xist*'s total upregulation. This conclusion is consistent with recent studies in which decreased DNase I hypersensitivity (Sado et al., 2005) and enriched RNA Pol II binding to the *Xist* promoter (Navarro et al., 2005) can be found in post-XCI cells. With an absolute copy number of only three to five RNAs per chromosome in pre-XCI cells, we suggest that *Xist* is effectively "off" in the pre-XCI state and that the low levels observed here and elsewhere (Beard et al., 1995; Lee et al., 1999) result from escape transcription. Our conclusions direct future research away from identifying RNA stabilization factors and toward finding transcriptional regulators.

The ability of the *Xist* P1 promoter to drive X/X-specific transcriptional activation supports the "two-factor" hypothesis for counting/choice (Lee, 2005). The one-factor theory proposes that a single "blocking factor" (BF) prevents XCI on one X per diploid cell and that *Xist* upregulation occurs on all remaining Xs by default. By contrast, the two-factor theory proposes that an additional "competence factor" (CF) is required to induce *Xist* on the Xi (Lee and Lu, 1999). We suggest that CF is part of the mechanism that bestows X/X-specific *Xist* activation.

Tsix RNA-Directed DNA Methylation as a Secondary Mechanism of *Xist* Regulation

Our present work has also shown that *Tsix* RNA forms a specific complex with the de novo DNA methyltransferase *Dnmt3a* (Okano et al., 1999). In differentiating female cells, loss of *Tsix* on one X leads to a rapid loss of *Xist* promoter methylation in *cis* and a concomitant gain of methylation on the homolog, consistent with recent results in post-XCI mouse embryos (Sado et al., 2005). Loss of *Tsix* on both Xs likewise results in a hypomethylation of *Xist*, in accordance with aberrant biallelic *Xist* expression during differentiation (Lee, 2005). We suggest that X^{Δ}/X^{Δ} inviability is due partly to deficient allelic methylation and *Xist* silencing. Thus, *Tsix* controls methylation of the *Xist* promoter in X/X cells. By contrast, *Tsix* deficiencies do not affect *Xist* methylation or XCI in X/Y cells. The absence of CF in X/Y cells (Lee, 2005) may circumvent the need for regulatable DNA methylation to repress *Xist*.

In female cells, although the *Tsix* RNA-*Dnmt3a* complex is detectable before XCI, the promoter is only partially and mosaically methylated. In *Tsix*-deficient females, DNA methylation patterns are only modestly affected. These findings imply that *Tsix*-directed DNA methylation at the *Xist* promoter is not preemptive and acts only after XCI is initiated. As such, we suggest that *Tsix*-directed DNA methylation does not play a role during the "initiation phase" but is invoked only after XCI is underway, perhaps serving as a secondary mechanism of silencing. Furthermore, *Tsix*'s role at this time is more likely to induce, rather than to recruit de novo, the methyltransferase activity of *Dnmt3a*. Indeed, *Dnmt3a* can be detected by DNA ChIP at the *Xist* promoter before XCI and even in *Tsix*-deficient cells (data not shown). Consistent with RNA-directed methylation being a secondary mechanism of *Xist* repression, knocking out *Dnmt3a* causes *Xist* to be demethylated without becoming transcriptionally activated (Sado et al., 2004).

A Transient Heterochromatic State Induces *Xist* Activation and Determines Choice

We propose that the primary mechanism of monoallelic *Xist* expression works through histone modification. We

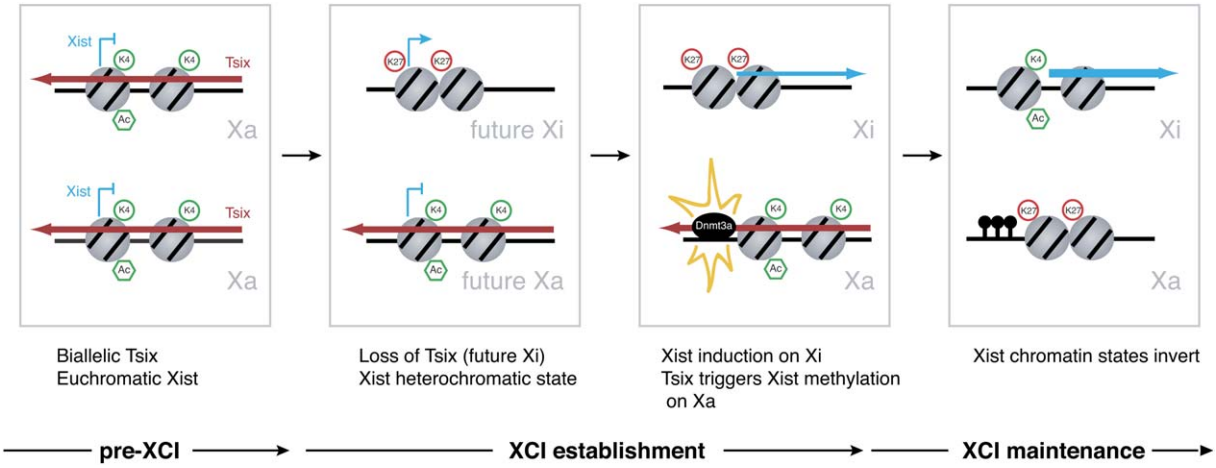

Figure 6. Model: Preemptive Histone Modifications Underlie Asymmetric *Xist* Activation

Before XCI, biallelic expression of *Tsix* maintains *Tsix*/*Xist* in a euchromatic state, as indicated by biallelic H3-K4 dimethylation and H4 acetylation. The euchromatic state precludes *Xist* transcription on both Xs. At the onset of XCI, silencing of *Tsix* on one X leads to heterochromatin in *Tsix*/*Xist* in *cis*, as indicated by loss of H3-2meK4 and H4 acetylation, gain of H3-3meK27, and activation of *Xist*. During the establishment of Xi, *Tsix* RNA activates *Xist* DNA methylation (lollipops) to lock *Xist* in a silent state. After XCI occurs, the *Xist* chromatin pattern inverts.

have identified modifications that precede and predict allelic choice and shown that *Tsix* directs the dynamic changes. On the future Xi, *Tsix* repression leads to preemptive histone H4 hypoacetylation (promoter), hypermethylation of H3-K27 (promoter and gene body), and hypomethylation of H3-K4 (gene body) on the *Xist* allele destined to be expressed. On the future Xa, persistent *Tsix* expression prevents the acquisition of these marks.

We propose that *Tsix* downregulation, a change in chromatin structure in *Xist*, and *Xist* transcriptional induction are three distinct sequential events (Figure 6). Prior to the onset of XCI, *Tsix* expression on both Xs establishes euchromatin in the two *Xist* alleles (low H3-3meK27, high H3-2meK4, high H4 acetylation). This open chromatin paradoxically inhibits *Xist* transcription, keeping *Xist* "off" with low-level escape transcription. At the onset of XCI, the persistence of *Tsix* expression maintains the euchromatic state and ensures continued *Xist* silence on the Xa. *Tsix* RNA may trigger *Dnmt3a* activity as a secondary mechanism of *Xist* silencing. On the Xi, downregulation of *Tsix* results in heterochromatin through *Tsix*/*Xist* (high H3-3meK27, low H3-2meK4, low H4 acetylation), which in turn enables transcriptional induction of *Xist*. Once XCI occurs, the *Xist* chromatin undergoes further change, perhaps in response to recruitment of additional factors by the newly expressed *Xist* RNA. During the maintenance phase, the *Xist* chromatin inverts to the low H3-3meK27/high H3-2meK4/high H4 acetylation configuration more typically associated with expressed loci.

Our model posits that *Tsix* serves as the binary switch for *Xist* and XCI by controlling the asymmetry of chromatin modification. The model is consistent with the various effects of *Xist* and *Tsix* mutants on X inactivation choice. Heterozygous *Xist* knockouts result in nonrandom inactivation of the remaining wt X (Marahrens et al., 1998; Penny et al., 1996). In such cells, we suggest that the loss of *Tsix* causes heterochromatinization of *Xist* in *cis*, but if the linked allele was defective, a feedback mechanism would enable the remaining X to make an attempt at silencing. By contrast, heterozygous *Tsix* mutants favor silencing of the mutated X. In this case, deleting *Tsix* predisposes the mutated X to silencing due to the establishment of preemptive heterochromatin at *Xist* even before the onset of XCI (Figure 5). In homozygous *Tsix* mutants, differentiating EBs display a mixture of 0, 1, or 2 Xi. In this case, loss of *Tsix* would cause heterochromatinization on both Xs, which predisposes to the induction of both *Xist* alleles. At the same time, however, the presence of only one "competence factor" would favor induction of only one *Xist* allele. These competing influences may explain why homozygous cells can show 1 Xi or 2 Xi's.

Finally, we note that our data have implications for two recent publications (Navarro et al., 2005; Sado et al., 2005). Using ChIP assays, Sado et al. concluded that low H3-3meK27 designates the active *Xist* allele, whereas Navarro et al. concluded that high H3-2meK4 in the *Xist* promoter determines the active *Xist* allele—exactly the opposite of our current conclusions. We believe that the discrepancy can be explained by the differing approaches. First, the prior two works carried out the critical experiments in cells of the post-XCI phase where the initiating marks may have been long erased. Notably, a state of low H3-3meK27 and high H3-2meK4 is precisely what we observe on the active *Xist* allele in post-XCI cells but is dramatically different from what we observe during the initiation phase. A second major difference lies in the use of X/Y versus X/X lines. There is an emerging understanding that X/X and X/Y lines may differ in some aspects of XCI, such as their differential ability to induce the *Xist* promoter in a reporter assay (Figure 3), promoter methylation patterns in the undifferentiated state (Figure 4), and differential response to mutations in X chromosome counting and choice (Lee, 2005; Lee and Lu, 1999; Ogawa and Lee, 2003). Furthermore, our analysis in X/X lines made possible the use of allele-specific ChIP for direct quantitation of methylation differences between the Xa and Xi, with each ChIP readout of the Xi being internally controlled by the Xa.

In conclusion, we have shown that *Tsix* functions as a binary switch for *Xist* transcription by controlling the asymmetric marking of chromatin. Our data imply that some of the critical factors reside within the *Xist* promoter, as the promoter by itself partly confers female-specific gene activation in ES cells. Our data argue that such transcription factors may prefer a heterochromatic environment. Thus, *Xist* may belong to the rare class of genes, such as *Light* of *D. melanogaster* (Wakimoto and Hearn, 1990), that require a heterochromatic setting to achieve full expression.

Experimental Procedures

Cell Lines and Culture

Wt male (J1), female (16.7), and *Tsix* mutant (CG7, 3F1, and ΔF10) ES lines, fibroblasts, and culture conditions have been described (Lee, 2002; Lee and Lu, 1999).

Plasmids, Primers, and Probes

All nucleotide positions are relative to the *Xist* P1 promoter start site (Brockdorff et al., 1992). pGEM7 (Promega) was the vector backbone unless noted. Probes for nuclear run-on are as follows: *Xist*, ssDNA of pπXB4 (6948/9424); *Tsix*, pBS1 (30884/34711); *Gapdh*, pBS3 (566/1017 of accession NM_008084); and *18SRNA* probe, pBS6 (1577/1727 of accession X00686). Probes for RNase protection are as follows: *Xist*, p*Xist3′* (*Xist* cDNA from 12527/14323 in pBluescript KS); *Tsix*, pNS2 (34434/34711); and Actin, pTRI-Actin (Ambion). Plasmids for competitive RT-PCR are as follows: pBS9 (−182/+2379); and pBS10 (pBS9 with BlpI-NdeI deletion). Plasmids for luciferase assay are as follows: pNS11, pNS42, and pNS258 as described (Stavropoulos et al., 2005). Primers are as follows: XP-2F, 5′-GCATAGACAGGTGTGTGCTA-3′; XP-3F, 5′-CGTCATGTCA CTGAGCTTAC-3′; XP-3R, 5′-GAGAGACCAGAAGAGGAGTG-3′; XP-4F, 5′-CTCCTCTTCTGGTCTCTCCG-3′; X1-17R, 5′-GAGAAAC CACGGAAGAACCG-3′; X1-22F, 5′-CGCTGCGCTAGCTAAAGGCT-3′; X1-23R, 5′-CTGAGCAGCCCTTAAAGCCAC-3′; X1-31F, 5′-GTGCT CTATACGTGGCGGTG-3′; X1-33R, 5′-CAGTGCTGGCTAAATAGA GG-3′; X1-36R, 5′-ACCGCACATCCACGGGAAACG-3′; X7-3F, 5′-GC CCATAATGGGAAGAGTAC-3′; X7-4R, 5′-GGCTCAAGTGGTCCTG TTGC-3′; X7-7F, 5′-CCTCCTTTCTGTTCACTTTGAGC-3′; and X7-10R, 5′-GGCGTTCACTTCAGAGCCACTTG-3′.

RNase Protection Assays

Assays were performed with the RPA-III kit (Ambion). Twenty micrograms of total RNA were used per assay with a 10:1 cpm probe ratio of *Xist* or *Tsix*:Actin. Probe sizes for *Xist*, *Tsix*, and *β-Actin* were 549, 313, and 304 nt (unprotected) and 476, 281, and 245 nt (protected).

Real-Time and Allele-Specific PCR

Real-time PCR was performed on a Bio-Rad iCycler machine with SYBR-Green iQ Mix (Bio Rad). Standard curves were generated by amplification of 10-fold plasmid dilutions; copy numbers were interpolated from the standard curve. Except as noted, all RT reactions used strand-specific primers. Allele-specific PCR was performed as described (Stavropoulos et al., 2001).

Nuclear Run-On Assays

Assays were performed essentially as described (Ashe et al., 1997), except that RNA was isolated by Trizol (Invitrogen). Preparations were hybridized to slot blot-prepared probes on nylon membranes in UltraHyb (Ambion). Twenty micrograms of probe was used per slot except for 18sRNA (1 μg). Signals were quantitated by phosphorimaging (Molecular Dynamics).

Competitive RT-PCR

To generate the RNA competitor, pBS9 was digested with BlpI and NdeI to release a 38 bp fragment, then religated to create pBS10. pBS10 was linearized with PmlI and transcribed with T7 RNA polymerase. RNA was verified as a single band by electrophoresis and quantitated by UV spectrophotometry. Predicted RNA molecular weight was used to calculate and generate 10-fold molar dilutions of the competitor. Cells were counted by hemocytometer and divided into equal aliquots and suspended in Trizol (Invitrogen). Competitor RNAs were added directly to Trizol suspensions. Equal volumes of RNA preparations were reverse transcribed (primer X1-23R) then amplified for 35 cycles (primers X1-22F and X1-23R).

Xist Half-Life Assay

10^5 ES cells were dispensed into each well of a 24-well plate containing male feeders and grown for 2 days. Fresh media containing 5 μg/ml Actinomycin D was added. At each time point, media was aspirated and total RNA collected by direct addition of Trizol (Invitrogen). After DNase treatment (Ambion), RNA levels were quantitated by strand-specific, real-time RT-PCR (primers X1-31F and X1-33R). *Xist*/*Tsix* transcript levels were plotted against levels at time point zero. Actinomycin treatments were repeated at least twice for each cell line and time point, and real-time RT-PCR was performed in triplicate.

Luciferase Assays

The reporter constructs have been described (Stavropoulos et al., 2005). Thirty micrograms of linearized pNS11 (no promoter:luciferase), pNS42 (1.6 kb *EF-1α* promoter:luciferase), and pNS258 (−540/+9 of *Xist* P1 promoter:luciferase) was electroporated into 10^7 X/Y and X/X ES cells at 240 V, 900 μF in a BioRad GenePulser. After selection in 300 μg/ml G418 for 9 days, pools of 25–100 neomycin-resistant colonies were collected. For luciferase experiments, 2×10^5 cells were dispensed in replicates onto 60 mm^2 plates. Cells were differentiated by growth without leukemia inhibitory factor (LIF). At day 4, EBs were attached to 12-well plates for adherent growth. At each time point, embryoid bodies were collected in 250 μl of Glo Lysis Buffer (Promega). One-hundred microliters of the lysate was mixed with 100 μl of Steady-Glo reagent (Promega) in a 96-well black OptiPlate (Packard) and incubated for 5 min. Luminescence was measured with a Packard TopCount-NXT instrument. Luciferase levels were normalized to total protein as measured by a noninterfering protein assay (Geno Technology, Inc). To correct for the general reduction of transgene expression during differentiation, *Xist*-promoter luciferase readings were normalized to *EF-1α* promoter-driven luciferase expression. Levels were compared to luciferase activity at time zero. Three independent differentiation experiments were carried out with similar results.

ChIP and RNA-ChIP

ChIP was performed as described (Gilbert et al., 2000). Five micrograms of antibody was used per IP. For RNA-ChIP, the identical protocol was followed except that 100 U of SuperRNAsin (Ambion) was added to the SDS-lysis buffer and 20 U to each IP sample; reversal of crosslinking was reduced to 2 hr. Samples were treated with DNA-free (Ambion). Reverse transcription (primer XP-3F) was performed with Superscript II (Invitrogen) and the cDNA amplified for 38 cycles (primers XP-3F and XP-3R). Antibodies are as follows: *Dnmt1*, *Dnmt2*, *Dnmt3a*, *Dnmt3b*, *Dmnt3l*, and normal rabbit IgG (Santa Cruz: sc-20701, 20702, 20703, 20704, 20705, and 2027); histone H3, histone 3-2meK4, histone 3-2meK9, histone 3-3meK27, and Acetyl-histone H4, *Eed* (Upstate: 06-755, 07-030, 07-441, 07-449, 06-598, and 07-368). For ChIP, real-time PCR was performed at the *Xist* promoter with XP-3F/XP-3R and in the *Xist* gene body with X7-3F/X7-4R. Allele-specific PCR was performed at the *Xist* promoter with XP-3F/X1-17R and resolved with Tsp509I digestion, yielding 41, 47, and 136 bp (129 allele), and 41 and 183 bp (castaneus allele). Within the gene body, amplification of X7-7F/X7-10R was digested with MnlI, yielding 65, 81, and 134 bp (129), and 81 and 199 bp (castaneus). Digests were resolved on a 2.2% agarose gel, transferred to nylon membranes, and hybridized to end-labeled oligonucleotides. Intensities were determined by phosphorimaging.

Methylation-Sensitive Restriction Analysis

Ten micrograms of genomic DNA was digested with BstXI, SpeI, and the methylation-sensitive enzyme. The SpeI site is unique to the castaneus X. Digests were resolved on a 0.6% agarose gel, transferred to nylon membranes, and hybridized to a ^{32}P-dCTP labeled probe spanning nucleotides 245–1403. For methylation-sensitive PCR, genomic DNA was digested with EcoRI to reduce overall DNA sizes. Resulting DNA was split equally into two reactions, one of which

contained the methylation-sensitive enzyme. Reactions were subjected to triplicate real-time PCR assays with flanking primers, and the ΔCt value was calculated as the difference between the average amplification threshold of undigested versus digested samples. SacII was amplified with primers XP-4F and X1-36R. MluI was amplified with primers XP-2F and XP-3R.

Supplemental Data

Supplemental Data include one figure and can be found with this article online at http://www.molecule.org/cgi/content/full/21/5/617/DC1/.

Acknowledgments

We thank K. Huynh, J. Tsai, N. Xu, and all members of the laboratory for critical comments and discussion; N. Stavropoulos for pNS11, 42, and 258; S. Gilbert and L. Corey for technical advice; and L. Gehrke, M. Kuroda, T. Wu, and G. Gill for ongoing guidance. This work was supported by the Medical Scientist Training Program (B.K.S), the Howard Hughes Medical Institute, and the National Institutes of Health (J.T.L.).

Received: August 2, 2005
Revised: November 30, 2005
Accepted: January 19, 2006
Published: March 2, 2006

References

Ashe, H.L., Monks, J., Wijgerde, M., Fraser, P., and Proudfoot, N.J. (1997). Intergenic transcription and transinduction of the human beta-globin locus. Genes Dev. *11*, 2494–2509.

Beard, C., Li, E., and Jaenisch, R. (1995). Loss of methylation activates *Xist* in somatic but not in embryonic cells. Genes Dev. *9*, 2325–2334.

Brockdorff, N., Ashworth, A., Kay, G.F., McCabe, V.M., Norris, D.P., Cooper, P.J., Swift, S., and Rastan, S. (1992). The product of the mouse *Xist* gene is a 15 kb inactive X-specific transcript containing no conserved ORF and located in the nucleus. Cell *71*, 515–526.

Brown, C.J., Hendrich, B.D., Rupert, J.L., Lafreniere, R.G., Xing, Y., Lawrence, J., and Willard, H.F. (1992). The human XIST gene: analysis of a 17 kb inactive X-specific RNA that contains conserved repeats and is highly localized within the nucleus. Cell *71*, 527–542.

Buzin, C.H., Mann, J.R., and Singer-Sam, J. (1994). Quantitative RT-PCR assays show *Xist* RNA levels are low in mouse female adult tissue, embryos and embryoid bodies. Development *120*, 3529–3536.

Cao, R., Wang, L., Wang, H., Xia, L., Erdjument-Bromage, H., Tempst, P., Jones, R.S., and Zhang, Y. (2002). Role of histone H3 lysine 27 methylation in Polycomb-group silencing. Science *298*, 1039–1043.

Chen, T., Ueda, Y., Dodge, J.E., Wang, Z., and Li, E. (2003). Establishment and maintenance of genomic methylation patterns in mouse embryonic stem cells by *Dnmt3a* and *Dnmt3b*. Mol. Cell. Biol. *23*, 5594–5605.

Clemson, C.M., Chow, J.C., Brown, C.J., and Lawrence, J.B. (1998). Stabilization and localization of *Xist* RNA are controlled by separate mechanisms and are not sufficient for X inactivation. J. Cell Biol. *142*, 13–23.

Gilbert, S.L., Pehrson, J.R., and Sharp, P.A. (2000). XIST RNA associates with specific regions of the inactive X chromatin. J. Biol. Chem. *275*, 36491–36494.

Goto, Y., Gomez, M., Brockdorff, N., and Feil, R. (2002). Differential patterns of histone methylation and acetylation distinguish active and repressed alleles at X-linked genes. Cytogenet. Genome Res. *99*, 66–74.

Johnston, P.G., and Cattanach, B.M. (1981). Controlling elements in the mouse. IV. Evidence of non-random X-inactivation. Genet. Res. *37*, 151–160.

Lavorgna, G., Dahary, D., Lehner, B., Sorek, R., Sanderson, C.M., and Casari, G. (2004). In search of antisense. Trends Biochem. Sci. *29*, 88–94.

Lee, J.T. (2002). Homozygous *Tsix* mutant mice reveal a sex-ratio distortion and revert to random X-inactivation. Nat. Genet. *32*, 195–200.

Lee, J.T. (2003). Molecular links between X-inactivation and autosomal imprinting: X-inactivation as a driving force for the evolution of imprinting. Curr. Biol. *13*, R242–R254.

Lee, J.T. (2005). Regulation of X-chromosome counting by *Tsix* and *Xite* sequences. Science *309*, 768–771.

Lee, J.T., and Lu, N. (1999). Targeted mutagenesis of *Tsix* leads to nonrandom X inactivation. Cell *99*, 47–57.

Lee, J.T., Davidow, L.S., and Warshawsky, D. (1999). *Tsix*, a gene antisense to *Xist* at the X-inactivation centre. Nat. Genet. *21*, 400–404.

Luikenhuis, S., Wutz, A., and Jaenisch, R. (2001). Antisense transcription through the *Xist* locus mediates *Tsix* function in embryonic stem cells. Mol. Cell. Biol. *21*, 8512–8520.

Lyon, M.F. (1961). Gene action in the X-chromosome of the mouse (Mus musculus L.). Nature *190*, 372–373.

Marahrens, Y., Loring, J., and Jaenisch, R. (1998). Role of the *Xist* gene in X chromosome choosing. Cell *92*, 657–664.

McDonald, L.E., Paterson, C.A., and Kay, G.F. (1998). Bisulfite genomic sequencing-derived methylation profile of the xist gene throughout early mouse development. Genomics *54*, 379–386.

Morey, C., Arnaud, D., Avner, P., and Clerc, P. (2001). *Tsix*-mediated repression of *Xist* accumulation is not sufficient for normal random X inactivation. Hum. Mol. Genet. *10*, 1403–1411.

Navarro, P., Pichard, S., Ciaudo, C., Avner, P., and Rougeulle, C. (2005). *Tsix* transcription across the *Xist* gene alters chromatin conformation without affecting *Xist* transcription: implications for X-chromosome inactivation. Genes Dev. *19*, 1474–1484.

Nesterova, T.B., Johnston, C.M., Appanah, R., Newall, A.E., Godwin, J., Alexiou, M., and Brockdorff, N. (2003). Skewing X chromosome choice by modulating sense transcription across the *Xist* locus. Genes Dev. *17*, 2177–2190.

Norris, D.P., Patel, D., Kay, G.F., Penny, G.D., Brockdorff, N., Sheardown, S.A., and Rastan, S. (1994). Evidence that random and imprinted *Xist* expression is controlled by preemptive methylation. Cell *77*, 41–51.

Ogawa, Y., and Lee, J.T. (2003). *Xite*, X-inactivation intergenic transcription elements that regulate the probability of choice. Mol. Cell *11*, 731–743.

Okano, M., Bell, D.W., Haber, D.A., and Li, E. (1999). DNA methyltransferases *Dnmt3a* and *Dnmt3b* are essential for de novo methylation and mammalian development. Cell *99*, 247–257.

Panning, B., Dausman, J., and Jaenisch, R. (1997). X chromosome inactivation is mediated by *Xist* RNA stabilization. Cell *90*, 907–916.

Penny, G.D., Kay, G.F., Sheardown, S.A., Rastan, S., and Brockdorff, N. (1996). Requirement for *Xist* in X chromosome inactivation. Nature *379*, 131–137.

Rougeulle, C., Chaumeil, J., Sarma, K., Allis, C.D., Reinberg, D., Avner, P., and Heard, E. (2004). Differential histone H3 Lys-9 and Lys-27 methylation profiles on the X chromosome. Mol. Cell. Biol. *24*, 5475–5484.

Sado, T., Tada, T., and Takagi, N. (1996). Mosaic methylation of *Xist* gene before chromosome inactivation in undifferentiated female mouse embryonic stem and embryonic germ cells. Dev. Dyn. *205*, 421–434.

Sado, T., Wang, Z., Sasaki, H., and Li, E. (2001). Regulation of imprinted X-chromosome inactivation in mice by *Tsix*. Development *128*, 1275–1286.

Sado, T., Okano, M., Li, E., and Sasaki, H. (2004). De novo DNA methylation is dispensable for the initiation and propagation of X chromosome inactivation. Development *131*, 975–982.

Sado, T., Hoki, Y., and Sasaki, H. (2005). *Tsix* silences *Xist* through nodification of chromatin structure. Dev. Cell *9*, 159–165.

Sheardown, S.A., Duthie, S.M., Johnston, C.M., Newall, A.E., Formstone, E.J., Arkell, R.M., Nesterova, T.B., Alghisi, G.C., Rastan, S., and Brockdorff, N. (1997). Stabilization of *Xist* RNA mediates initiation of X chromosome inactivation. Cell *91*, 99–107.

Shendure, J., and Church, G.M. (2002). Computational discovery of sense-antisense transcription in the human and mouse genomes. Genome Biol. *3*, RESEARCH0044.

Shibata, S., and Lee, J.T. (2003). Characterization and quantitation of differential *Tsix* transcripts: implications for *Tsix* function. Hum. Mol. Genet. *12*, 125–136.

Shibata, S., and Lee, J.T. (2004). *Tsix* transcription- versus RNA-based mechanisms in *Xist* repression and epigenetic choice. Curr. Biol. *14*, 1747–1754.

Sleutels, F., and Barlow, D.P. (2002). The origins of genomic imprinting in mammals. In Homology Effects, J.C. Dunlap and C.-t. Wu, eds. (San Diego: Academic Press), pp. 119–154.

Stavropoulos, N., Lu, N., and Lee, J.T. (2001). A functional role for *Tsix* transcription in blocking *Xist* RNA accumulation but not in X-chromosome choice. Proc. Natl. Acad. Sci. USA *98*, 10232–10237.

Stavropoulos, N., Rowntree, R.K., and Lee, J.T. (2005). Identification of developmentally specific enhancers for *Tsix* in the regulation of X chromosome inactivation. Mol. Cell. Biol. *25*, 2757–2769.

Wakimoto, B.T., and Hearn, M.G. (1990). The effects of chromosome rearrangements on the expression of heterochromatic genes in chromosome 2L of Drosophila melanogaster. Genetics *125*, 141–154.

Wutz, A., and Jaenisch, R. (2000). A shift from reversible to irreversible X inactivation is triggered during ES cell differentiation. Mol. Cell *5*, 695–705.

Yelin, R., Dahary, D., Sorek, R., Levanon, E.Y., Goldstein, O., Shoshan, A., Diber, A., Siton, S., Tamir, Y., Khosravi, R., et al. (2003). Widespread occurrence of antisense transcription in the human genome. Nat. Biotechnol. *21*, 379–386.